HYDROGEN INFLUENCE ON EXPLOSIVE WELDED CORROSION RESISTANT CLAD MATERIALS FOR GEOTHERMAL PLANTS

M. Gloc[1], Ł.Ciupiński[1], G. Kwiatkowski[2]
michalgloc@wp.pl

[1] Warsaw University of Technology, University Research Centre Functional Materials; Warsaw, Poland
[2] ZTW Explomet Co. A.Gałka, Z.Szulc; Opole, Poland

Project „Novel explosive welded corrosion resistant clad materials for geothermal plants”

UCB University Research Centre – Functional Materials, Warsaw University of Technology, Poland

EXPLOMET High-Energy Techniques Works, Opole, Poland

ICI Innovation Center Iceland, Iceland

MR SAS Institute of Materials Research of Slovak Academy of Sciences, Slovakia

ExploGuard in Poland is funded by The National Centre for Research and Development according to the contract No. M-ERA.NET/2013/01/2015 dated. 01.29.2015 r. under the Programme M-ERA.NET "

Geothermal energy

- Depleting resources of fossil fuels and global warming effect lead to development of renewable energy sources like use of geothermal steam to produce electricity.

- Geothermal energy has been used for heating and electricity production in several countries. The use of geothermal energy is being constantly developed and is gaining more importance in the global energy mix.

- Widespread use of geothermal energy as well as exploration of deeper geothermal sources bring about new challenges in the area of corrosion and use of materials that directly influence the effectiveness, quality of service, reliability and economy of the power plants.

Material problems

- Hydrogen, dissolved CO_2, H_2S, NH_3 and Cl ions present in geothermal water lead to corrosion of metallic materials, scalling settlement and progressive degradation that in conjunction with applied stresses results in component failures.

- Fatigue tests conducted on different types of steels exploited in Icelandic geothermal systems have shown that the decrease in strength parameters and reduced materials life span can be attributed to stress corrosion cracking and hydrogen embrittlement

Goals

- **The aim of the work is to develop new materials obtained by connect at least two different metals with use of explosives. The developed materials will be applied in geothermal infrastructure components such as tanks and pipelines.**

- **Explosive technique allows obtaining materials with unique properties such as strength and resistance to degradation.**

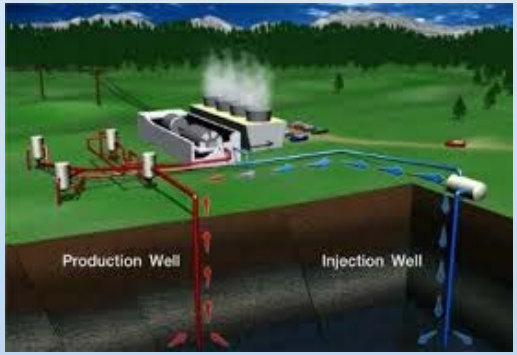

Development
of explosive welding technology of innovative clad coatings

Evaluation
of corrosion resistance of the innovative clad coatings

Characterization
of microstructure and properties of the innovative clad coatings using modern techniques

The idea

- Production of explosive welding joints by using different type of explosives, allowing a transition zone and interlayer formation in joint

- It lays in the explicate use of the inherent to explosive welding transition zones. Occurring in the joint transition zone and/or interlayer will constitute a diffusion barrier for hydrogen, which is one of the main factors triggering rapid degradation of the components.

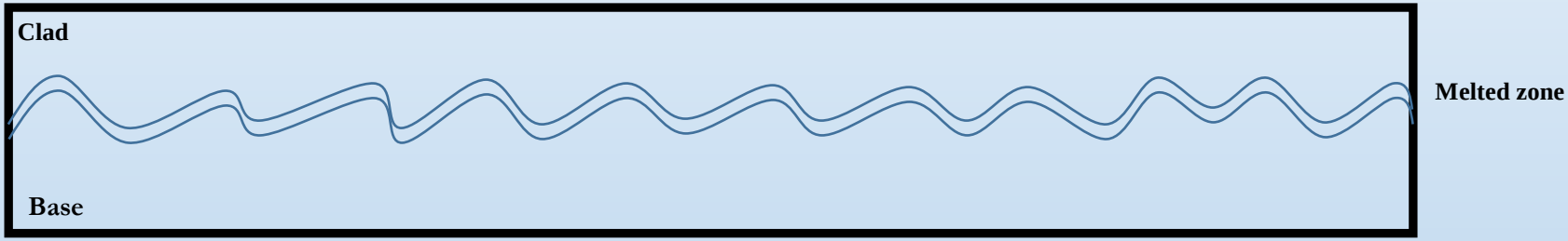

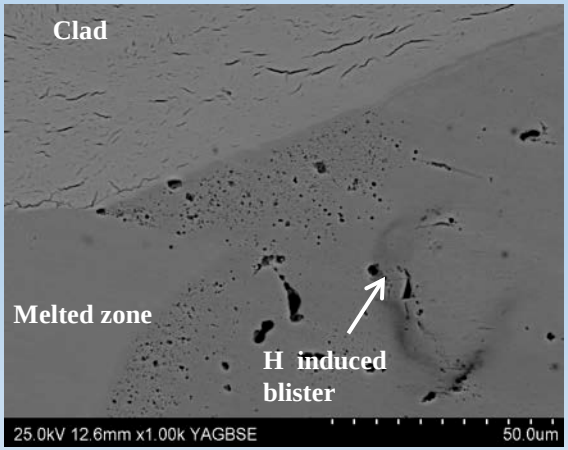

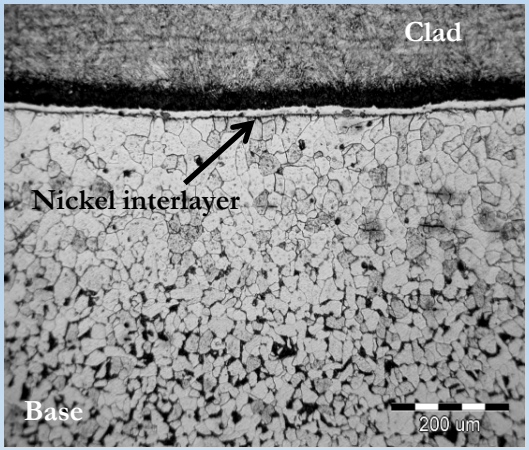

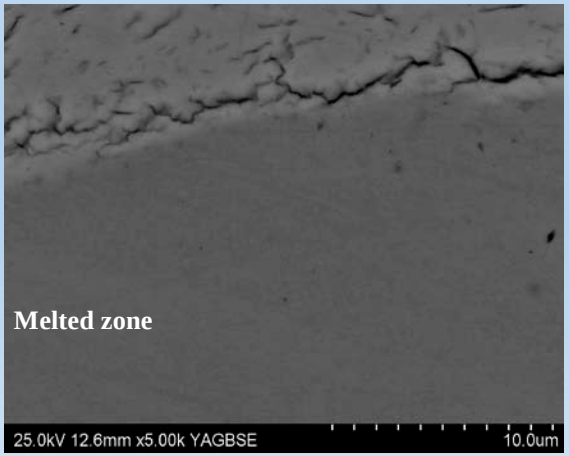

Materials joining

Joinig were conduct by EXPLOMET company (Opole Poland, www.explomet.pl)

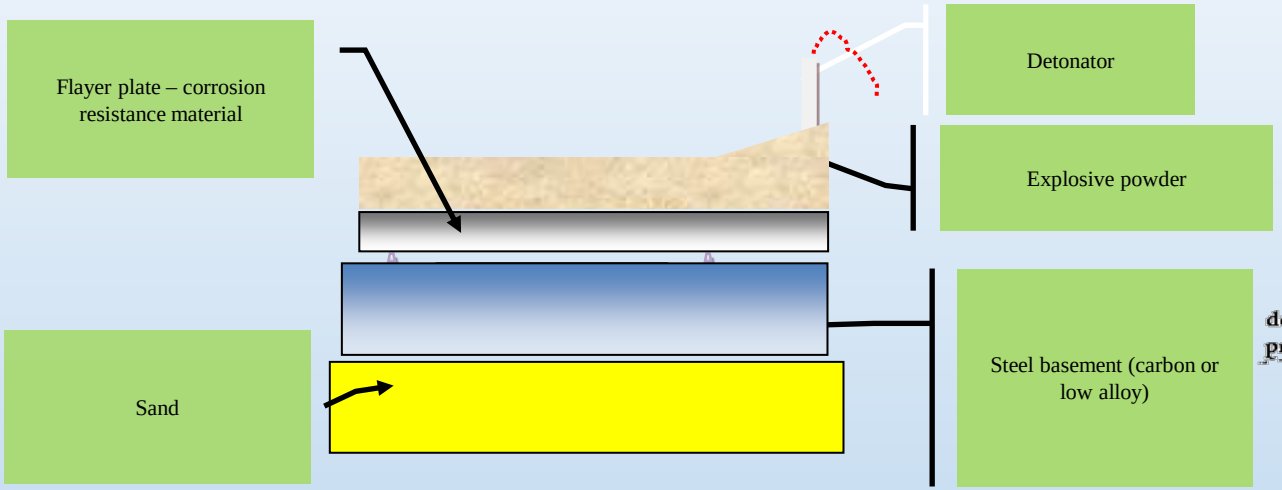

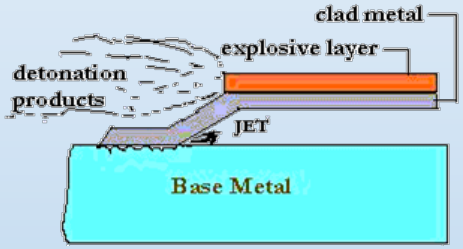

Two kinds of joint were produced:
„Normal parameters” and
„over parameters” to receive continuous interlayer between clad/base

Materials characterizations

- Samples preparations and processing of environmental samples for analysis is key to obtaining accurate, precise, and reliable information. UCB onsite sample preparation laboratory is equipped with all the instrumentation, supplies, and safety controls needed to prepare environmental samples for analysis.

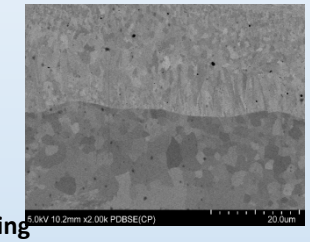

ION etcher for cross sectioning

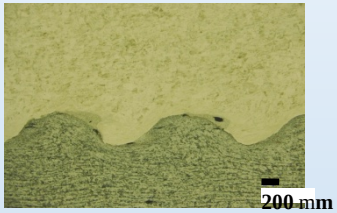

Electropolisher for samples preparation

Automatic polishers

- Microscopic observations were done by the variety of devices from light microscopies to SEM and TEM (inlc. PDBSE and BSE techniques), EDS chemical composition measurements techniques

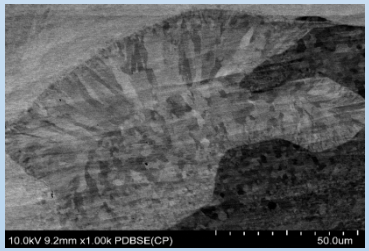

Hitachi SU 70 SEM

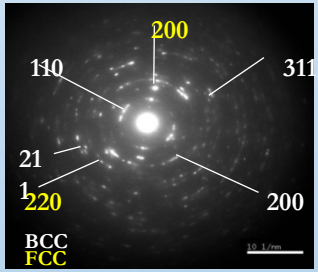

Hitachi 2700HD STEM

- Mechanical tests (shear test, microhardness test)

MTS 810

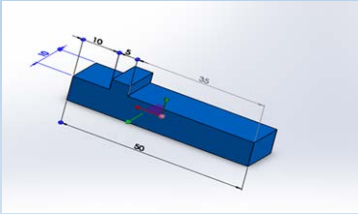

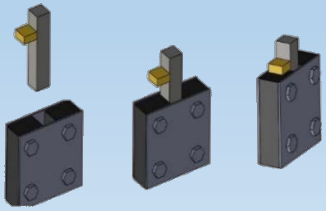

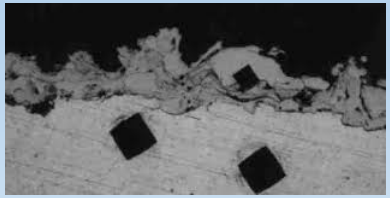

Materials for investigations

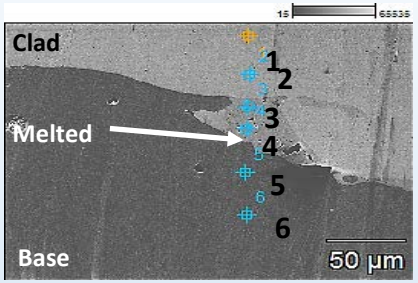

	C-K	Si-K	Cr-K	Mn-K	Fe-K	Ni-K	Mo-L
pt1	0.7	1.2	16.3	0.5	6.2	60.8	14.3
pt2	0.6	1.2	16.5	0.5	6.2	60.6	14.3
pt3	0.8	1.2	16.3	0.7	26.5	40.2	14.3
pt4	0.7	1.1	11.2	0.9	31.2	44.8	10.2
pt5	0.7	0.4	0.2	1.4	96.8	0.4	
pt6	0.7	0.5		1.4	97.1	0.3	

Sample 1.1 Base material: **P355NH**; Plate material: Inconel **C-276.** Chemical composition of base, clad, and melted zone

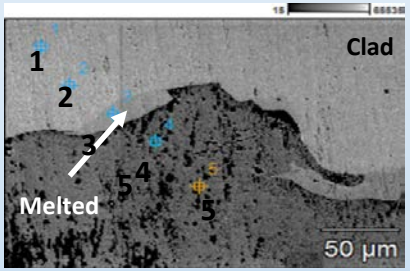

	C-K	Si-K	Cr-K	Mn-K	Fe-K	Ni-K	Mo-L
pt1	0.8	1.2	16.2	0.7	6.1	61.0	14.1
pt2	0.9	1.2	16.3	0.6	6.2	60.7	14.1
pt3	0.7	0.8	10.2	1.0	38.4	39.9	9.0
pt4	0.9	0.4		1.5	96.8	0.4	
pt5	1.0	0.4	0.1	1.7	96.8		

Sample 1.2 (annealed 610^{0}C) Base material: **P355NH**; Plate material: Inconel **C-276.** Chemical composition of base, clad, and melted zone

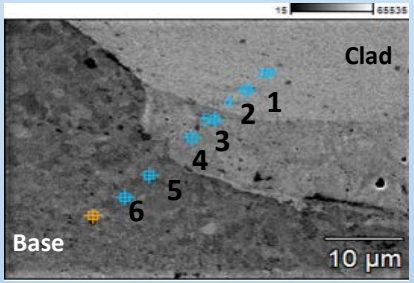

	C-K	Al-K	Si-K	Cr-K	Mn-K	Fe-K	Ni-K	Mo-L
pt1	0.6	0.1	0.5	26.3	1.3	61.6	5.5	4.0
pt2	0.6	0.2	0.4	23.5	1.5	62.9	8.3	2.6
pt3	0.6	0.1	0.5	25.8	1.2	63.0	5.1	3.7
pt4	0.6	0.2	0.3	0.6	1.4	97.7	4.2	
pt5	0.7	0.1	0.3		1.6	97.3		
pt6	0.8	0.2	0.4		1.5	97.1		

Sample 2.1, Base material: **P355NH**; Plate material: **SAF 2507,** austenitic-ferritic stainless steel. Chemical composition of base, clad, and melted zone

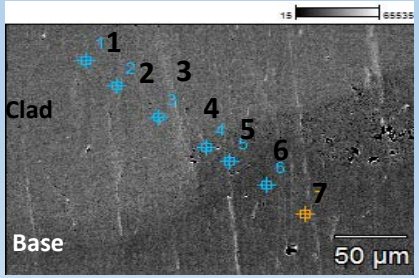

	C-K	Al-K	Si-K	Cr-K	Mn-K	Fe-K	Ni-K	Mo-L
pt1	0.7	0.1	0.4	23.8	1.3	63.1	7.8	2.7
pt2	0.5	0.2	0.6	29.4	1.4	58.2	7.1	5.6
pt3	0.6	0.1	0.4	22.6	1.2	64.8	7.8	2.5
pt4	0.6	0.2	0.6	16.2	1.4	74.0	4.7	2.3
pt5	0.5	0.1	0.5	17.1	1.3	73.1	5.1	2.3
pt6	0.7	0.1	0.4	0.2	1.4	97.1		
pt7	0.6	0.2	0.3		1.4	97.1		

Sample 2.2 (annealed 610^{0}C), Base material: **P355NH**; Plate material: **SAF 2507,** austenitic-ferritic stainless steel. Chemical composition of base, clad, and melted zone

Electrochemical corrosion testing

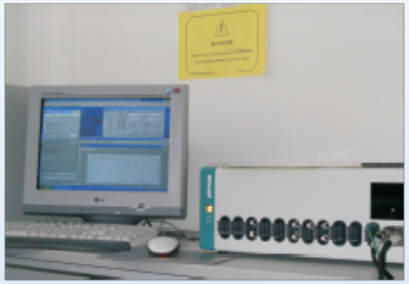

Electrochemical corrosion

AutoLab PGStat100

max. output current	± 250 mA
max. output voltage	± 100 V
current range	10 nA ÷ 100mA
frequency range	10 µHz ÷ 1MHz
Impedance	0.1 Ω ÷ 100 GΩ

Electrochemical corrosion

Atlas 99 EII

max. output current	± 2 A
max. output voltage	± 25 V
current range	2 µA ÷ 2 A
frequency range	10 mHz ÷ 100kHz
Impedance	0.1 Ω ÷ 10MΩ

LPS 305

max. output power	165 W
output voltage	± 30 V
setting resolution	10 mV
output current	± 2.5 A
setting resolution	1mA

System for hydrogen charging

Investigation methods

-Electrochemical impedance spectroscopy (EIS)
-Anodic polarization curves
-Linear polarization resistance
-Hydrogen cathodic charging
-Measurements of deformations in samples during hydrogen charging

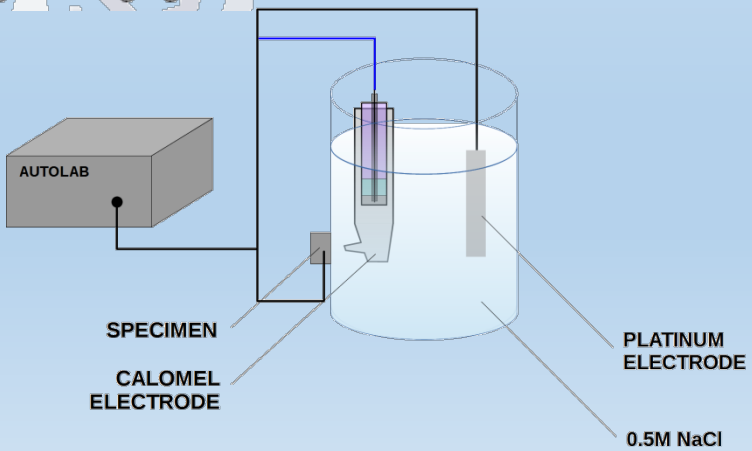

Electrochemical corrosion testing

C-276 Inconel; 0,004% C; <0,002% S; **16% Cr**; **57,96% Ni**; 0,47% Mn; 0,04% Si; 15,71% Mo; 0,01% Nb; 0,01% Cu; **5,78% Fe**; 0,04% P; 3,39%

Sample 1.1

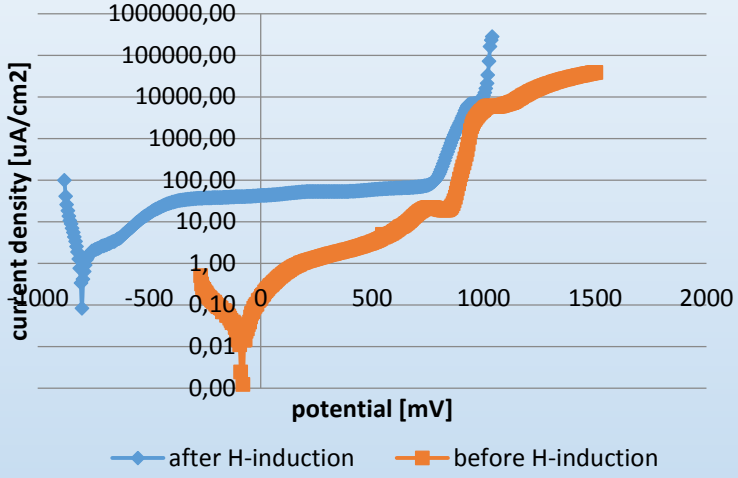

Before H-charging:
i_{cor}= 0,0125µA
E_{cor}= -94mV
E_{br}= 745mV
corrosionrate:
$2{,}903 \cdot 10^{-4} \frac{mm}{year}$

After H-charged:
i_{cor}= 0,5559µA
E_{cor}= -810mV
E_{br}=732mV
corrosionrate:
$1{,}291 \cdot 10^{-2} \frac{mm}{year}$

Sample 1.2 (annealed)

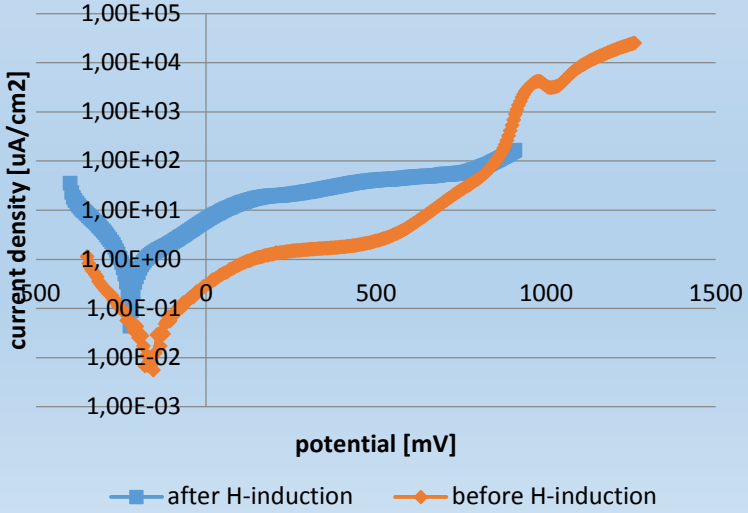

Before H-charging:
i_{cor}= 0,0121µA
E_{cor}= -186mV
E_{br}= 957mV
corrosionrate:
$2{,}799 \cdot 10^{-4} \frac{mm}{year}$

After H-charged:
i_{cor}= 0,3575µA
E_{cor}= -215mV
E_{br}=773mV
corrosionrate:
$8{,}304 \cdot 10^{-3} \frac{mm}{year}$

SAF 2507 Austenitic-ferritic stainless steel; 0,015% C; 0,37% Si; 0,83% Mn; 0,026% P; 0,001% S; 24,90% Cr; 6,89% Ni; 3,79% Mo; 0,33% Cu; 0,25% N

Sample 2.1

Before H-charged:
i_{cor}= 0,0532µA
E_{cor}= -179mV
E_{br}= 964mV
corrosionrate:
$2{,}497 \cdot 10^{-4} \frac{mm}{year}$

After H-charged:
i_{cor}= 0,8585µA
E_{cor}= -28mV
E_{br}=953mV
corrosionrate:
$1{,}994 \cdot 10^{-3} \frac{mm}{year}$

Sample 2.1 (annealed)

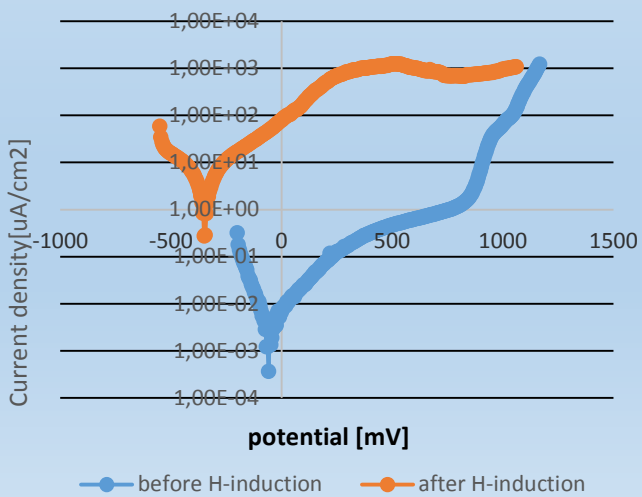

Before H-charged:
i_{cor}= 0,00172µA
E_{cor}= -66mV
E_{br}= 817mV
corrosionrate:
$3{,}994 \cdot 10^{-5} \frac{mm}{year}$

After H-charged:
i_{cor}= 2,304µA
E_{cor}= -352mV
corrosionrate:
$352 \cdot 10^{-2} \frac{mm}{year}$

Microstructural observations

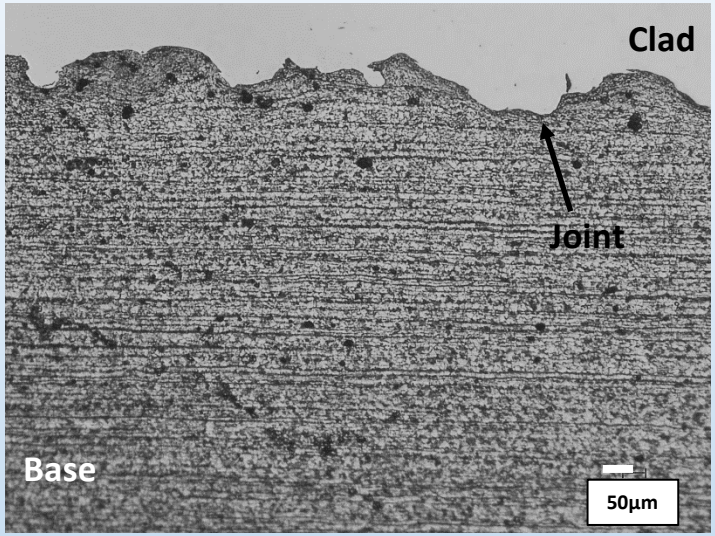

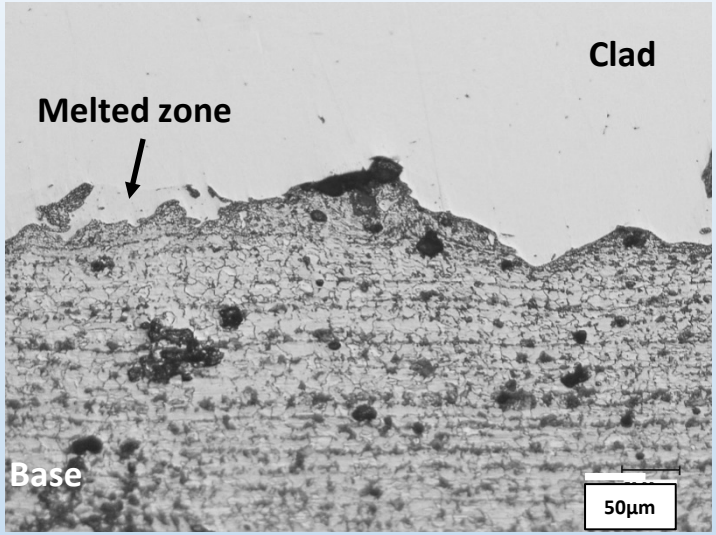

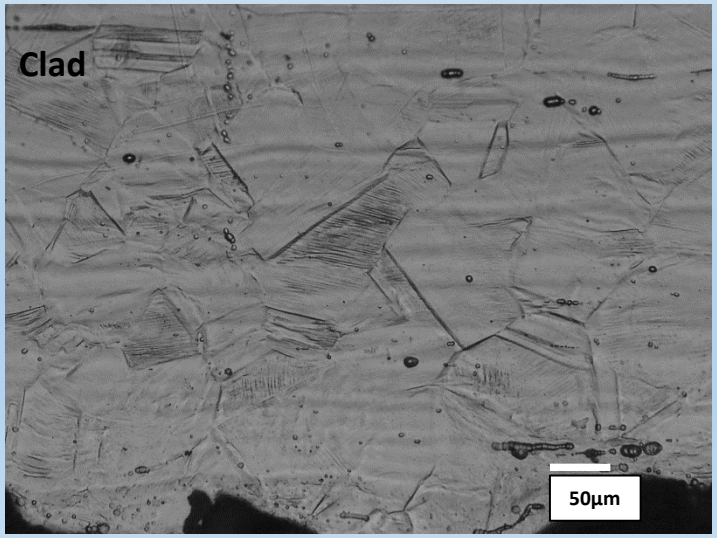

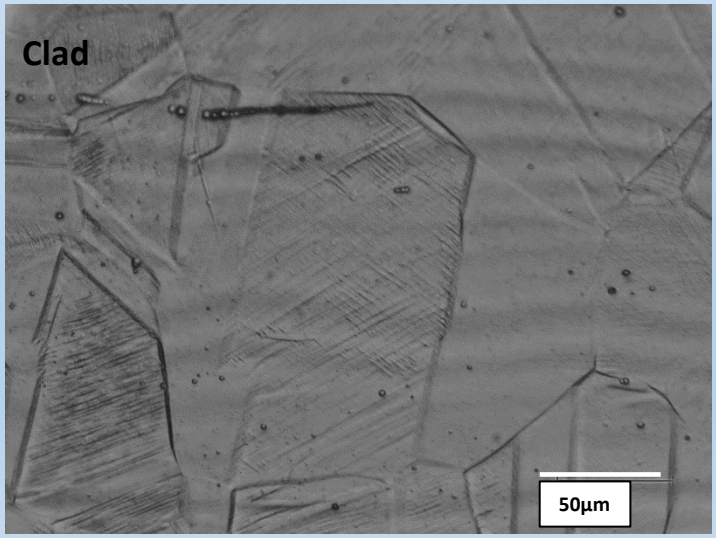

Sample 1.1 Base material: **P355NH**; Plate material: Inconel **C-276. LM**

Microstructural observations– ION etching

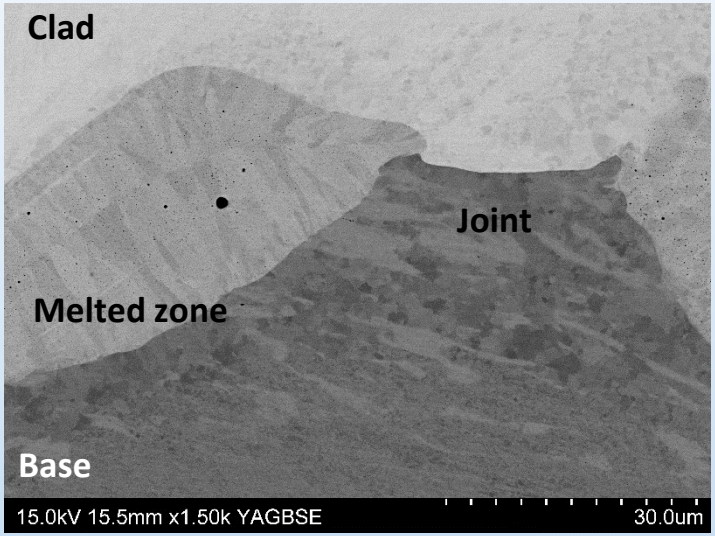

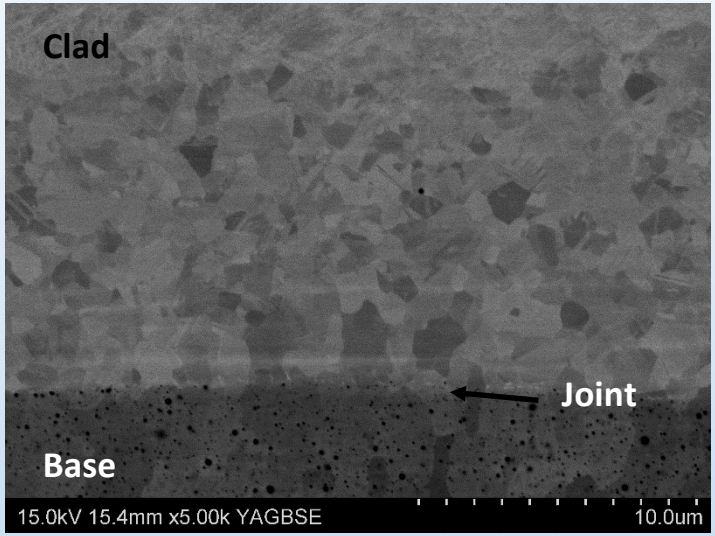

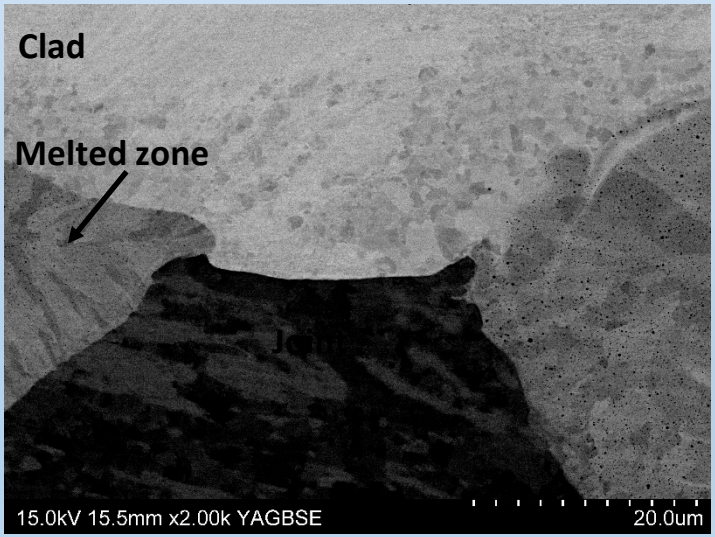

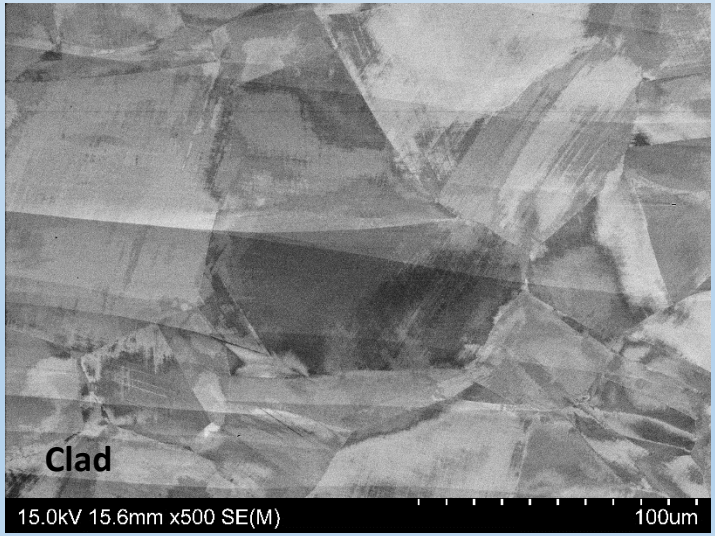

Sample 1.1 Base material: **P355NH**; Plate material: Inconel **C-276. SEM**

Microstructural observations

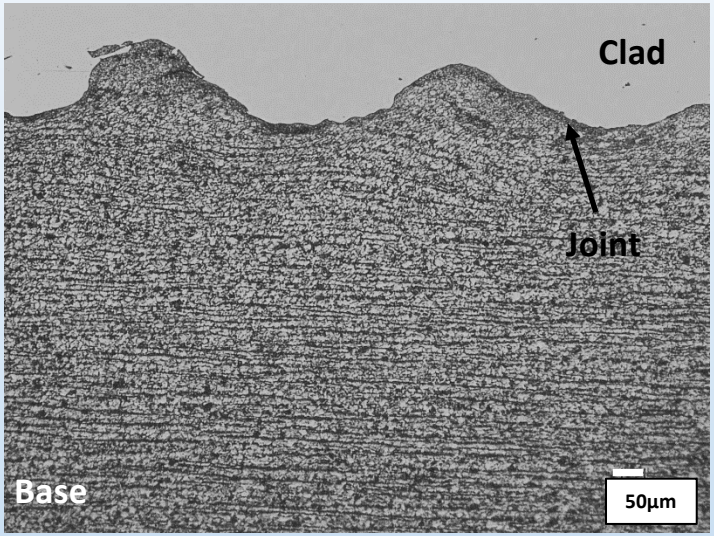

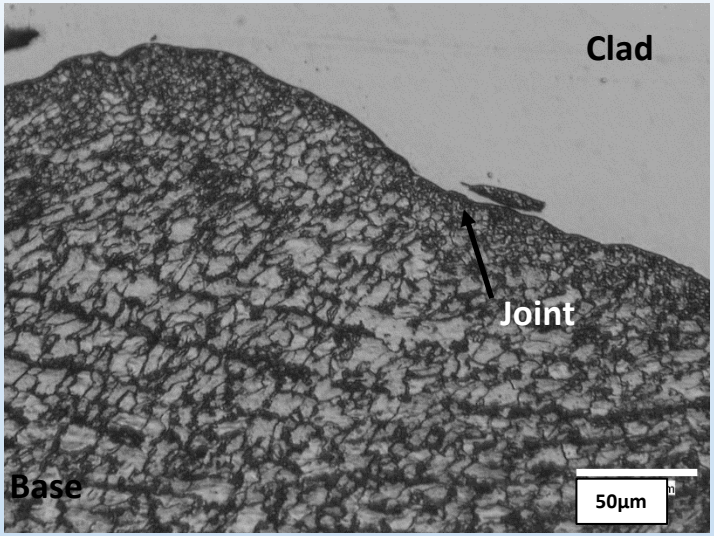

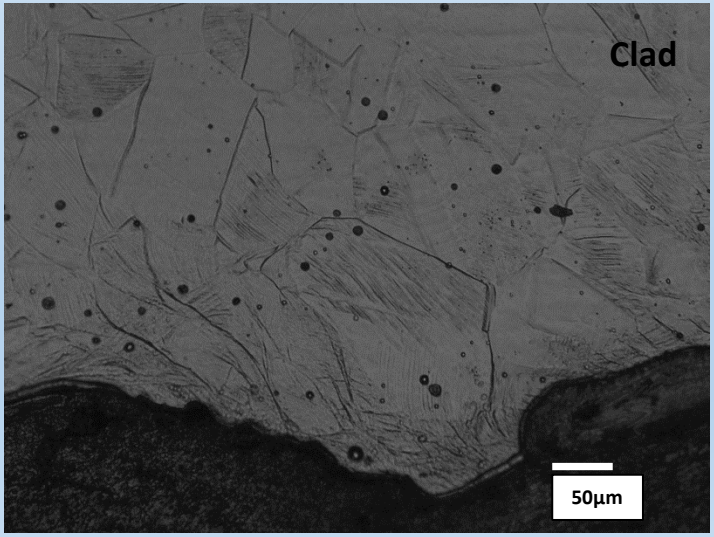

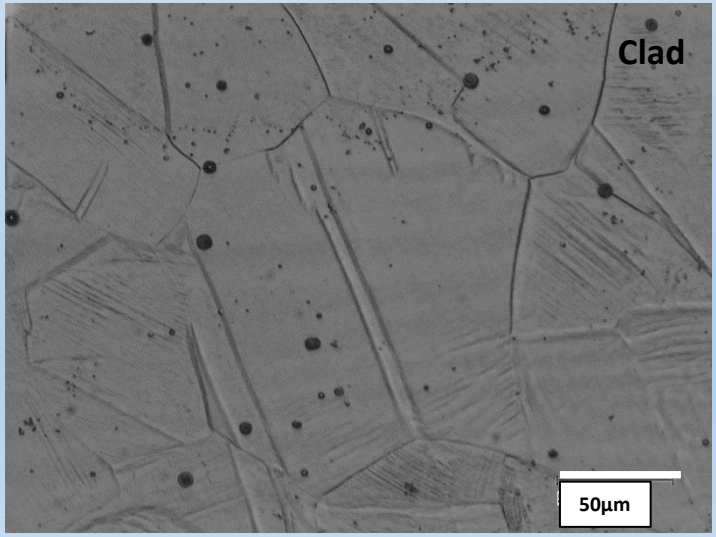

Sample 1.2 Base material: **P355NH**; Plate material: **C-276**, Inconel .**LM**

Microstructural observations– ION etching

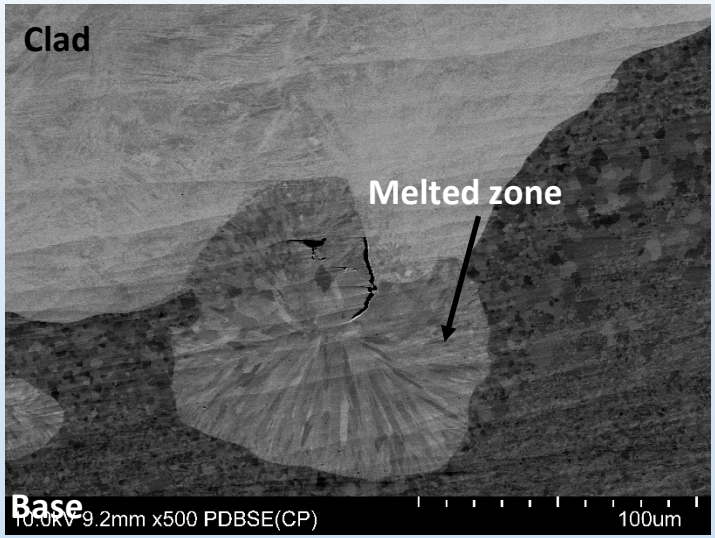

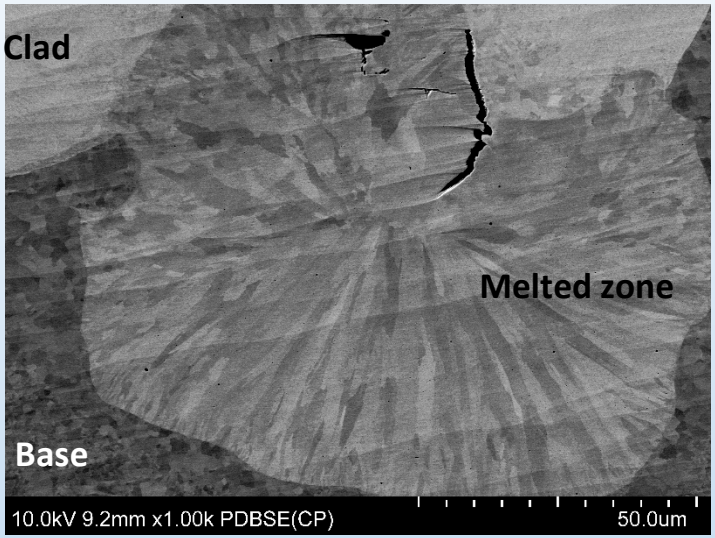

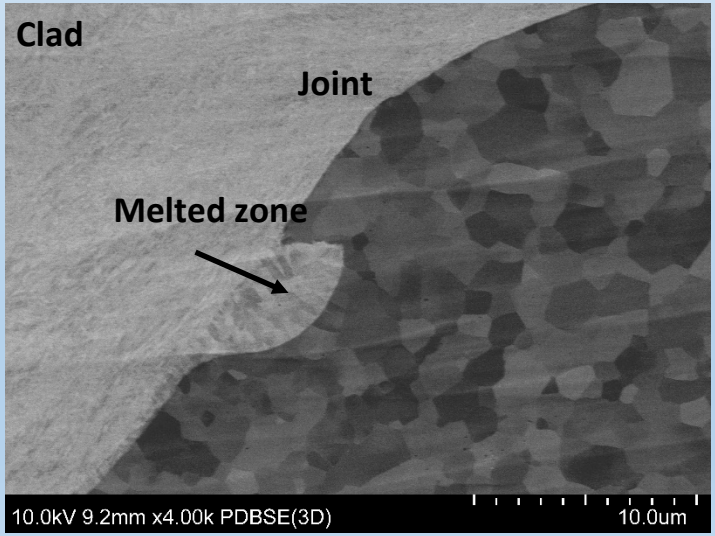

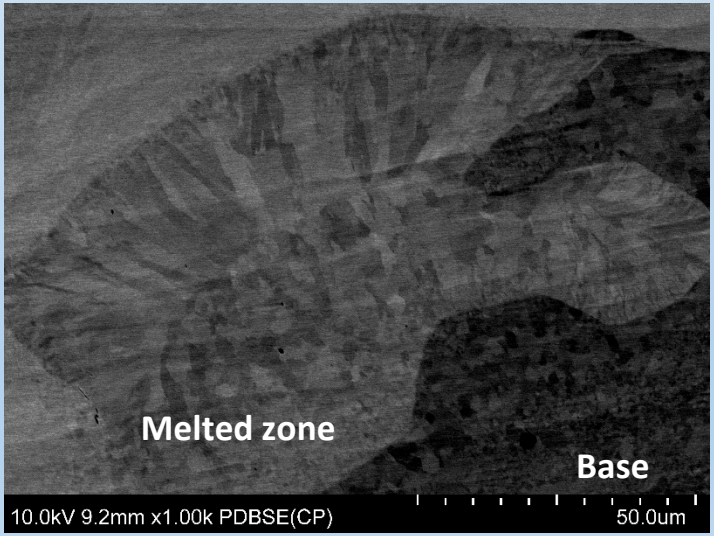

Sample 1.2 Base material: **P355NH**; Plate material: Inconel **C-276. Heat treatment. SEM**

Microstructural observations

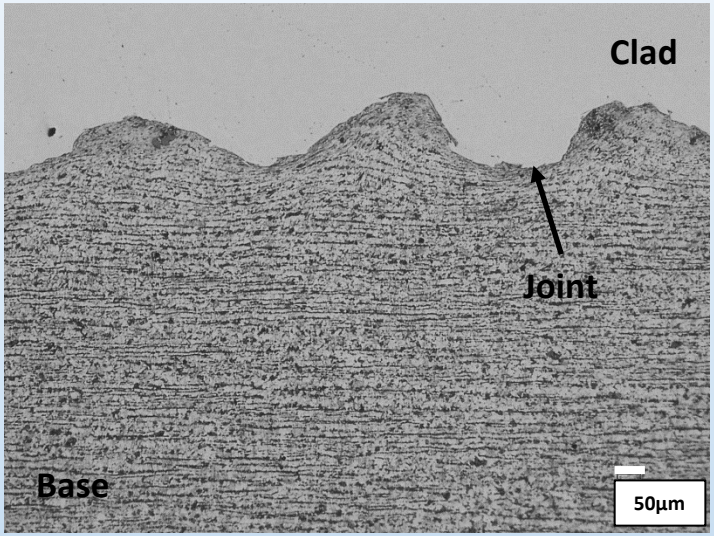

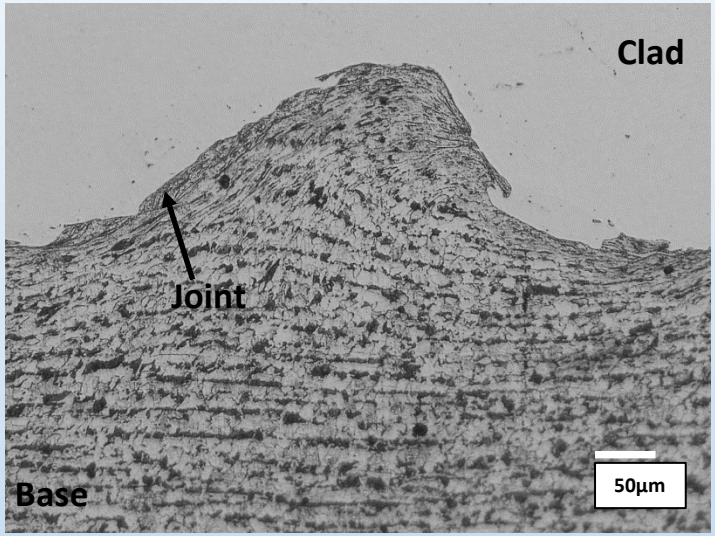

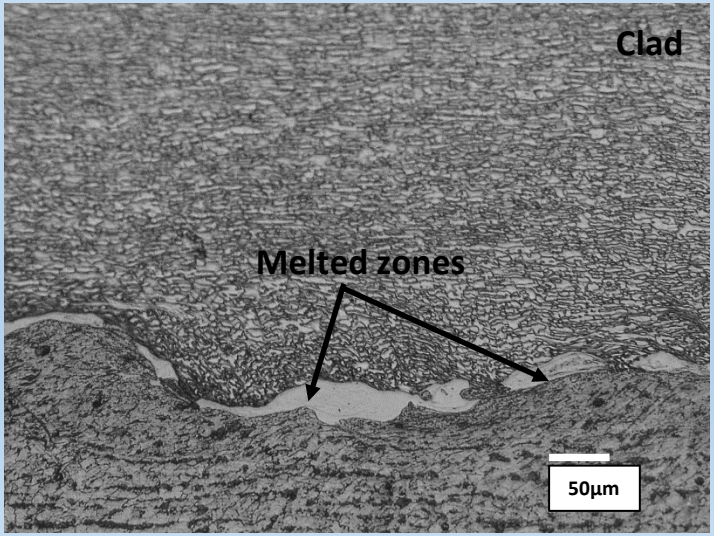

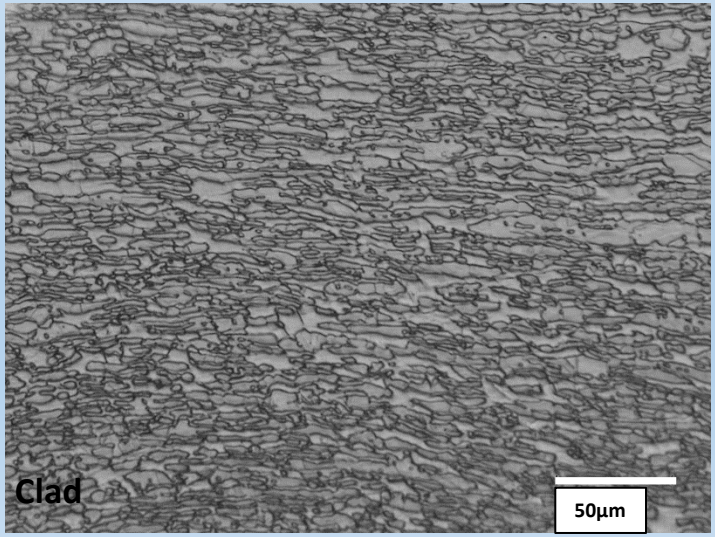

Sample 2.1, Base material: **P355NH**; Plate material: **SAF 2507,** austenitic-ferritic stainless steel. **LM**

Microstructural observations– ION etching

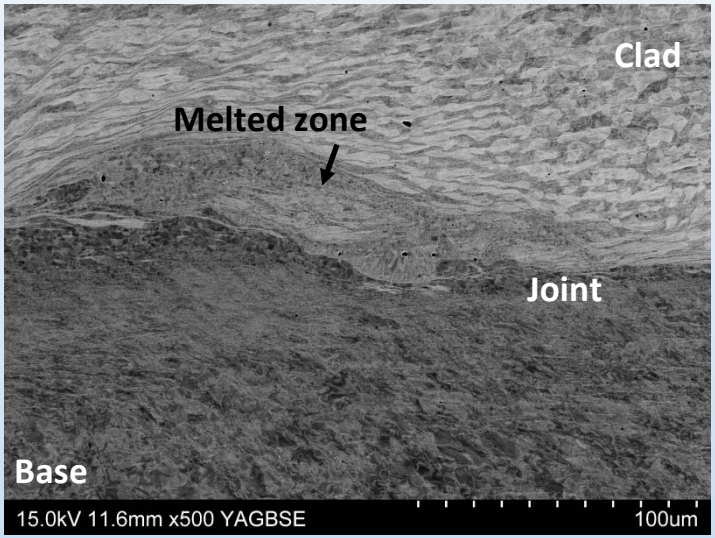

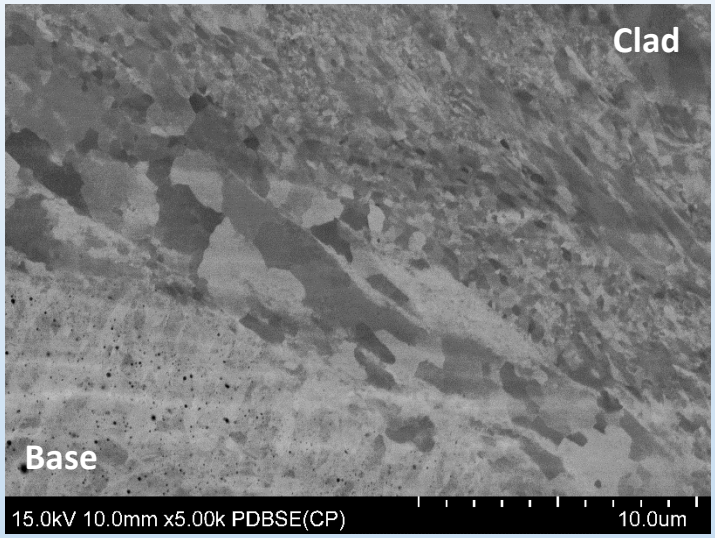

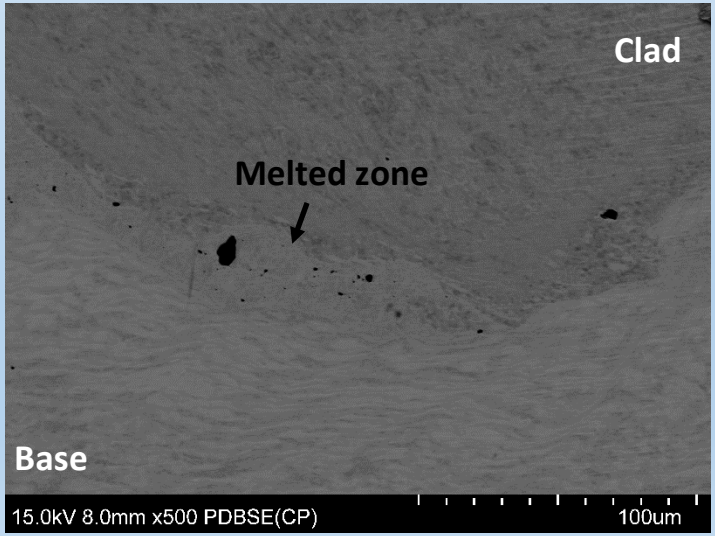

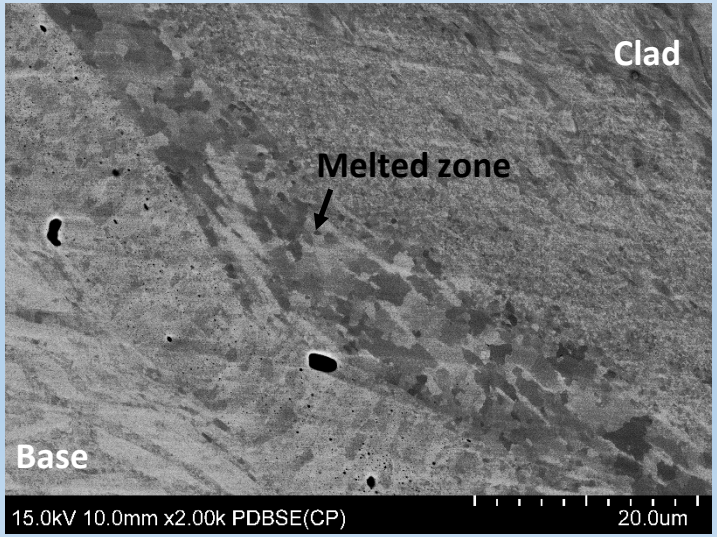

Sample 2.1, Base material: **P355NH**; Plate material: **SAF 2507,** austenitic-ferritic stainless steel. **SEM**

Microstructural observations

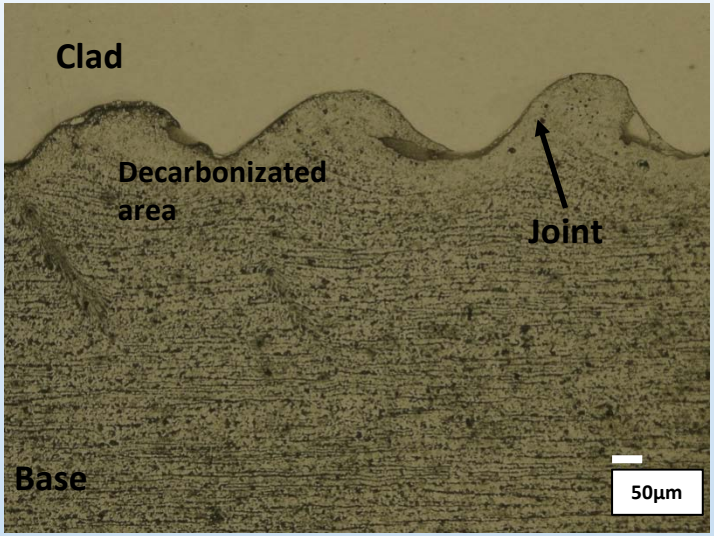

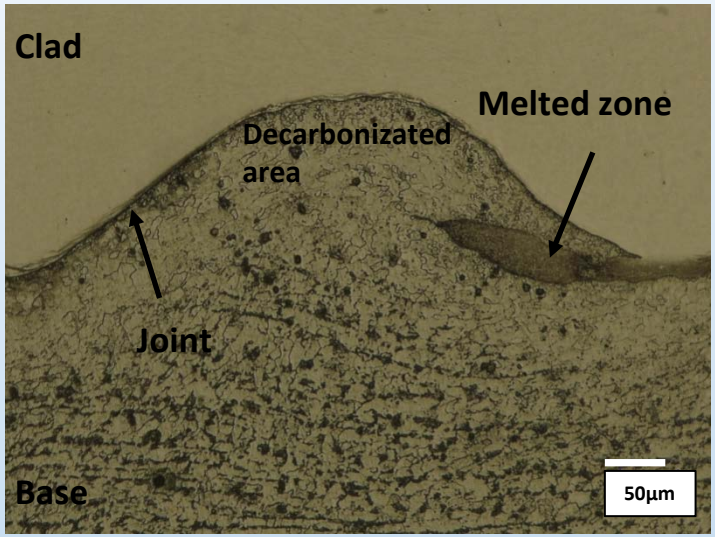

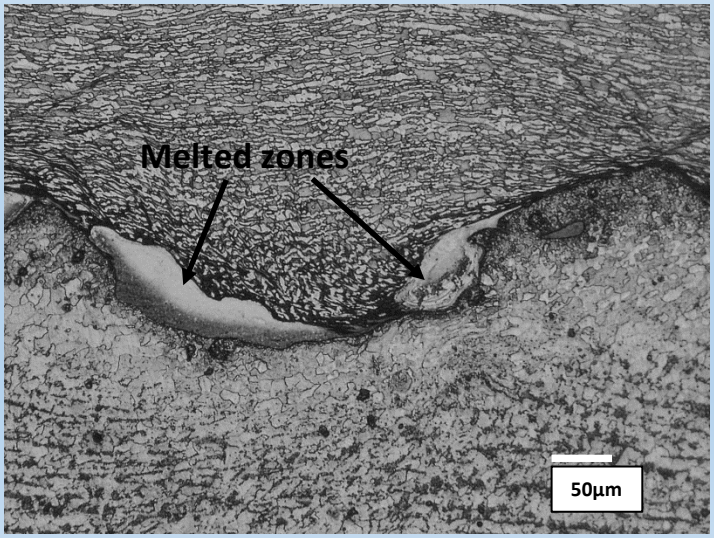

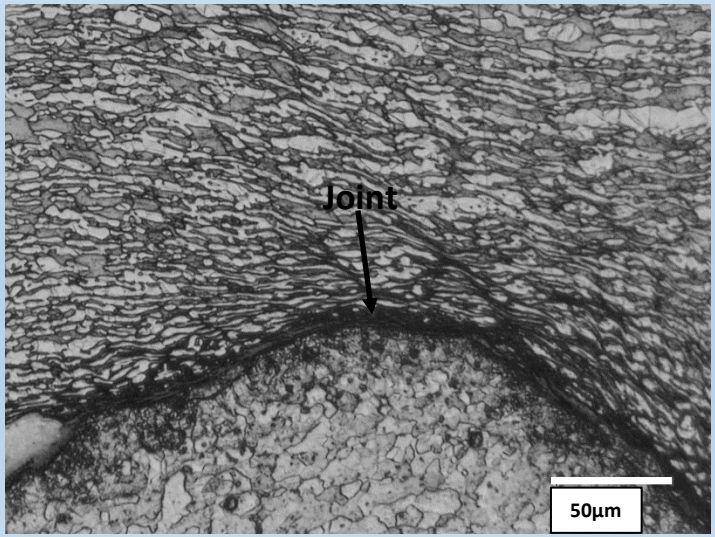

Sample 2.2, Base material: **P355NH**; Plate material: austenitic-ferritic stainless steel **SAF 2507. LM**

Microstructural observations– ION etching

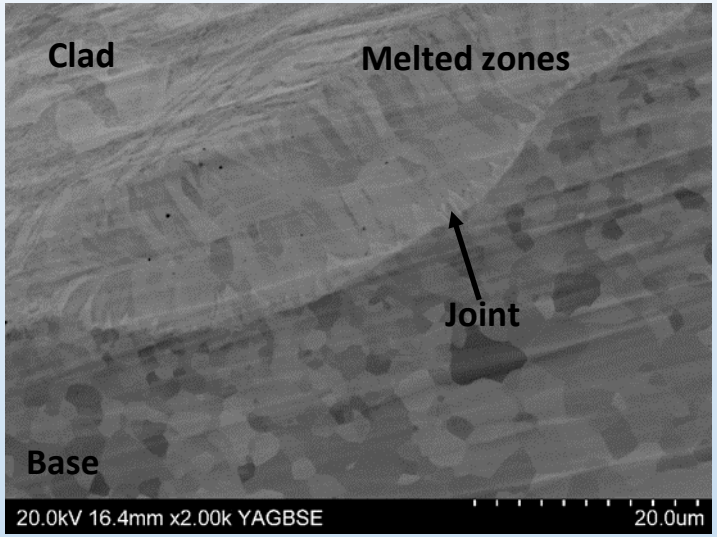

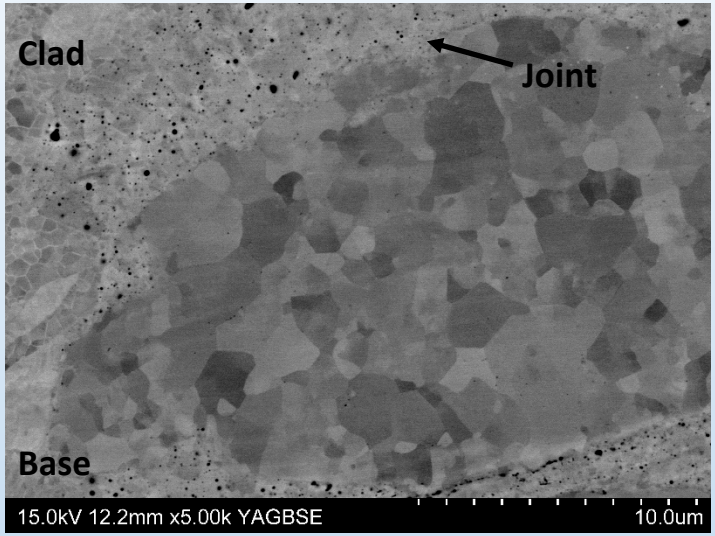

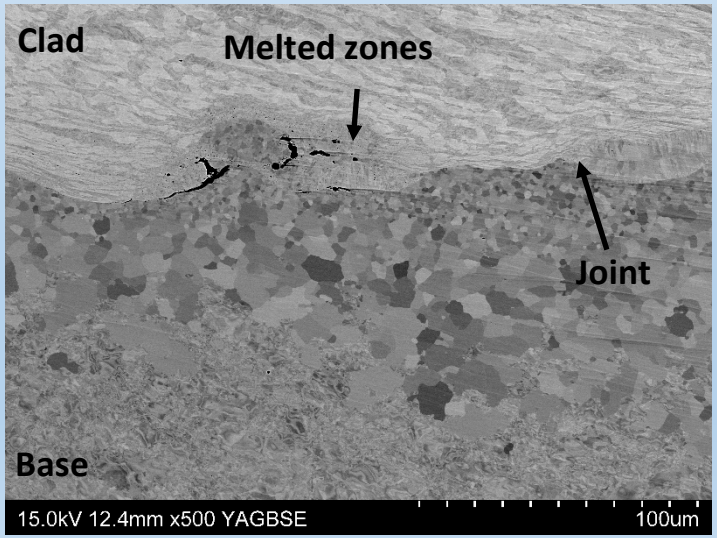

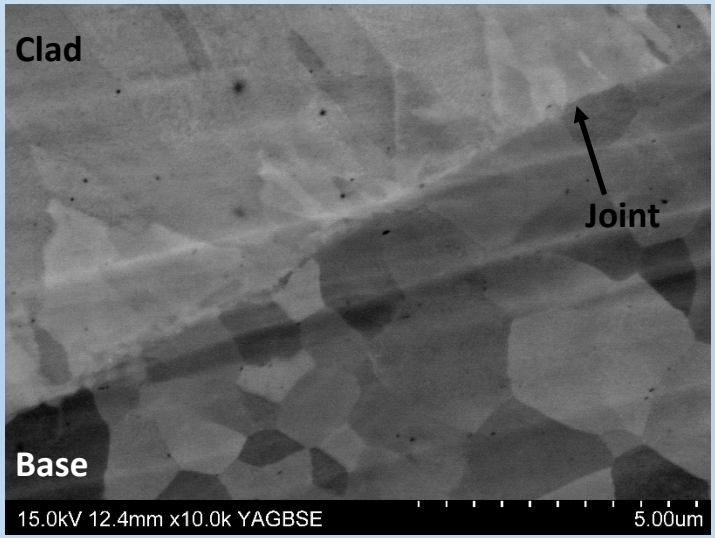

Sample 2.2, Base material: **P355NH**; Plate material: austenitic-ferritic stainless steel **SAF 2507.SEM**

Hydrogen charging

Hydrogen charging parameters:

- **0.5M H_2SO_4 solution, with addition hydrogen entry promoter**
- **ambient temperature**
- **current density: 50mA/cm^2**
- **time: 2 - 18 hours**

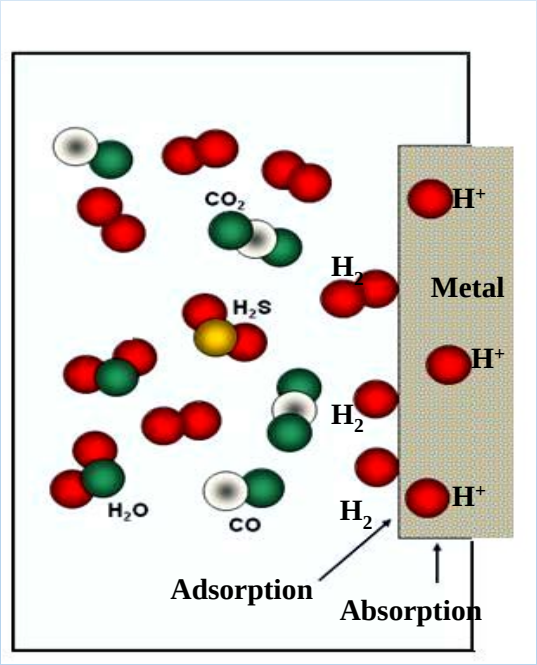

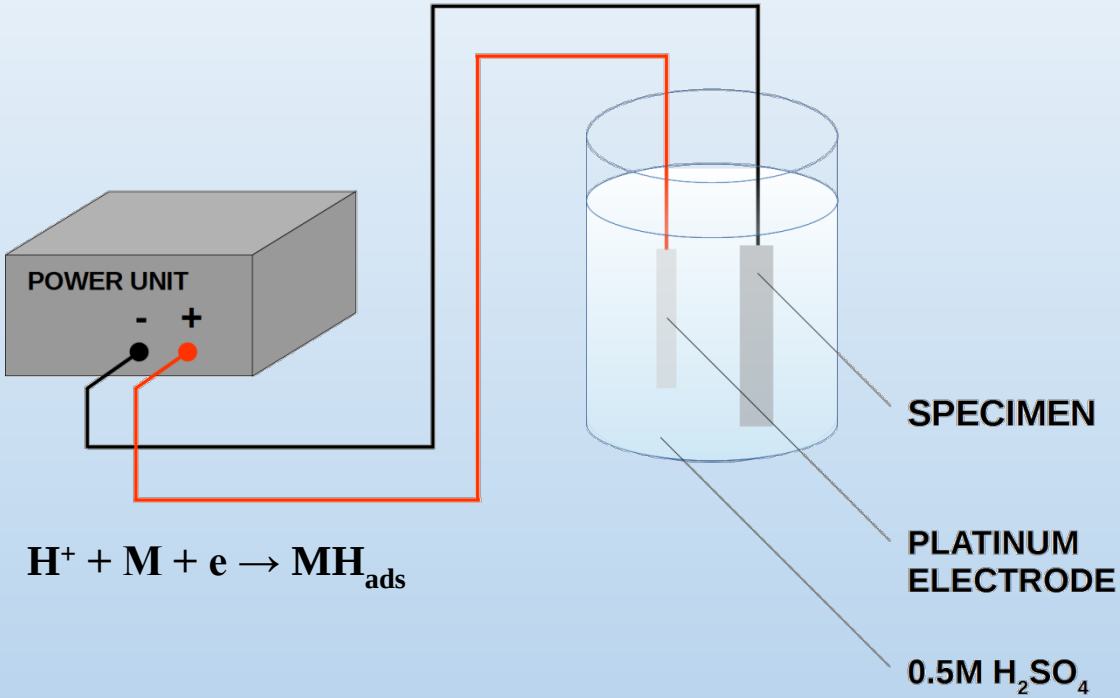

$$H^+ + M + e \rightarrow MH_{ads}$$

Hydrogen degradation of clad steels

FCC

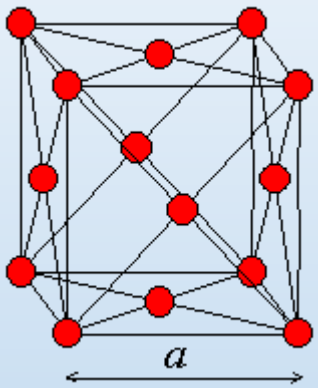

BCC

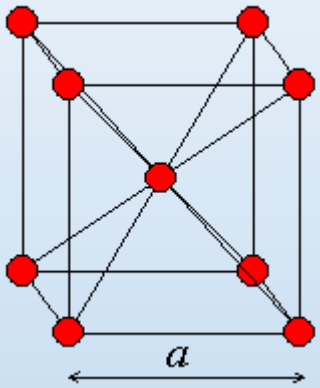

austenite			ferrite	
10^{-15} m^2/s	low	hydrogen diffusion coefficient	high	$8{,}46 \cdot 10^{-11}$ m^2/s
	high	hydrogen solubility	low	

LOCAL SUPERSATURATION OF HYDROGEN

DISBONDING

Hydrogen degradation of clad steels

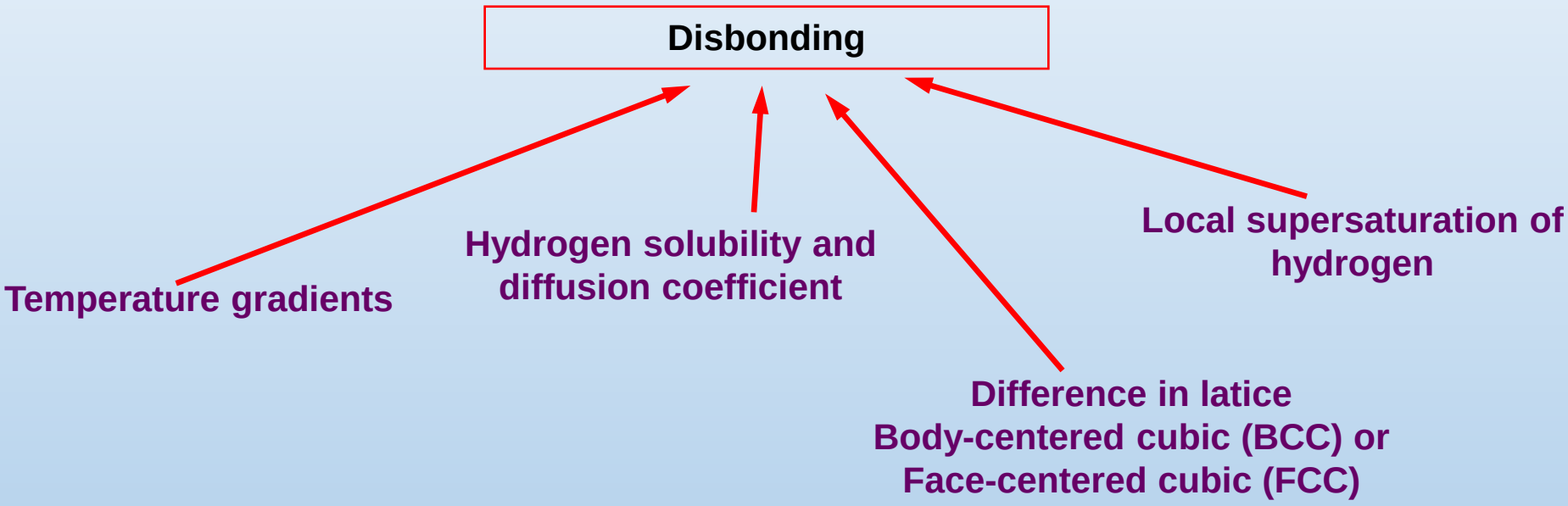

Microstructural observations after H charging

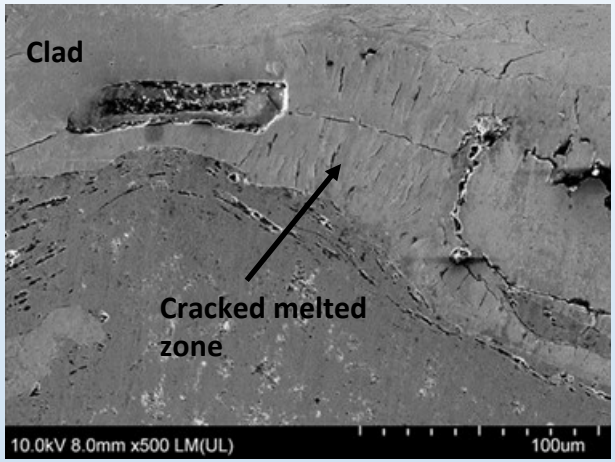

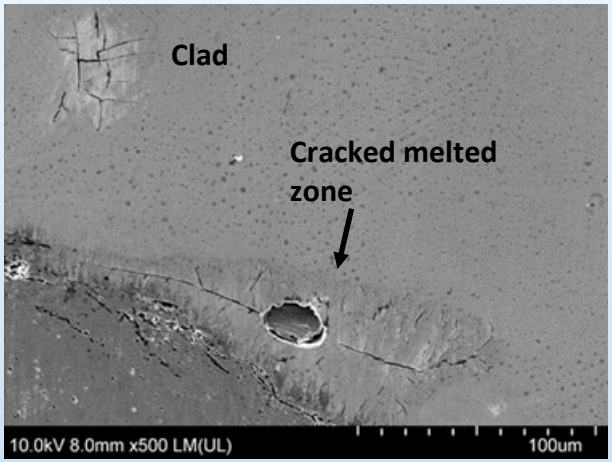

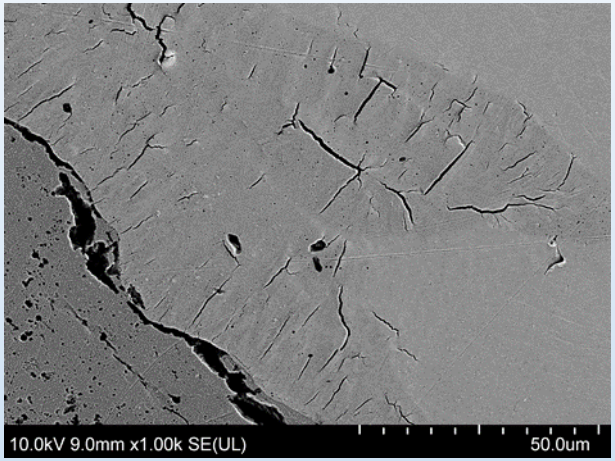

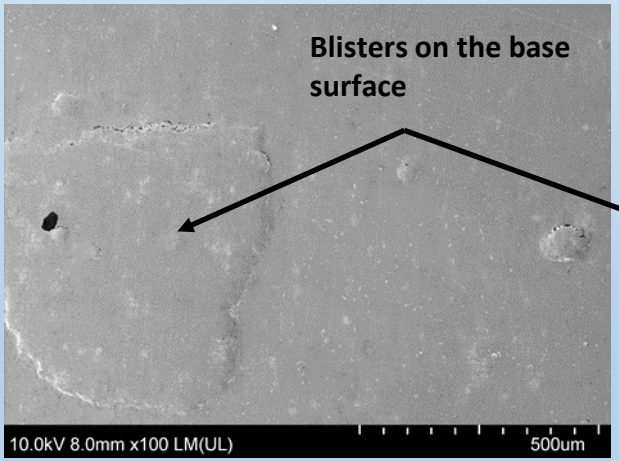

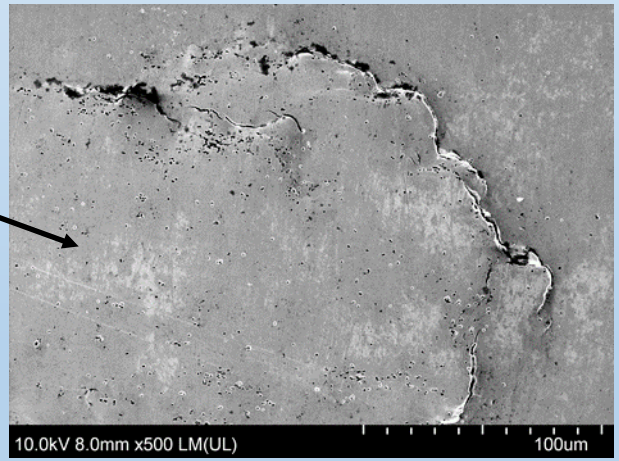

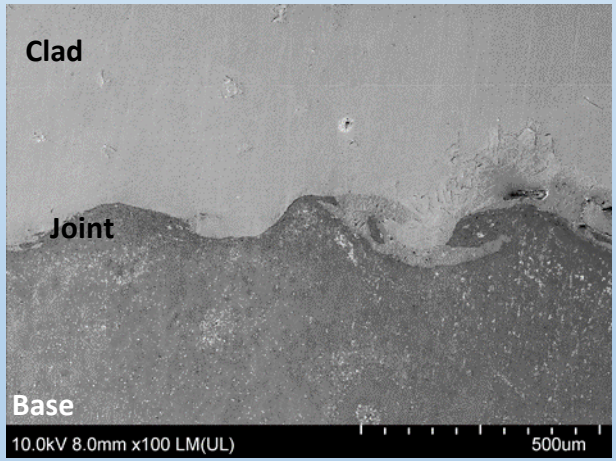

Sample 1.1 Base material: **P355NH**; Plate material: Inconel **C-276.** after hydrogen charging. Visible of cracked melted zones. Area of clad material (up to 500μm from the joint) remains unchanged

Microstructural observations after H charging

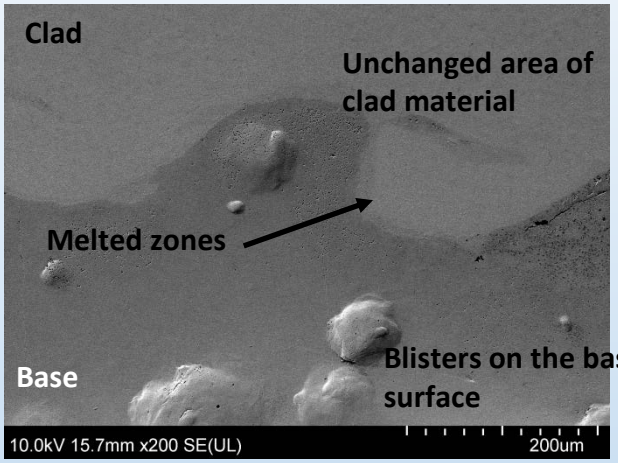

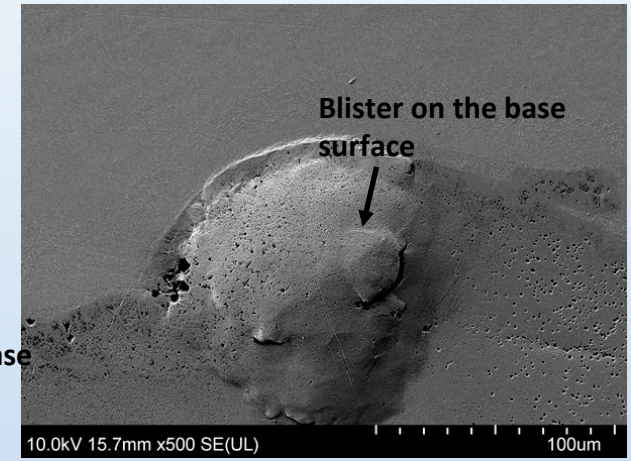

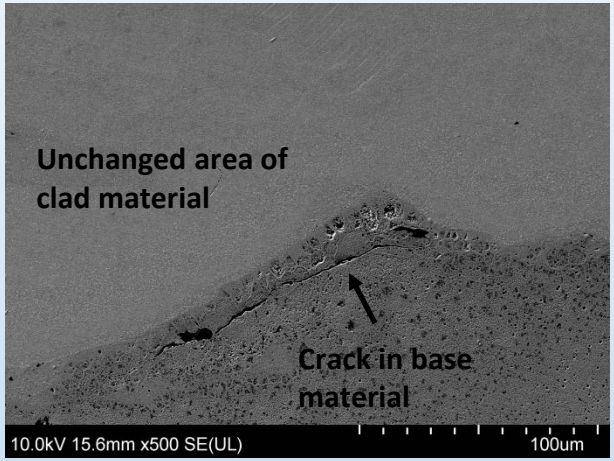

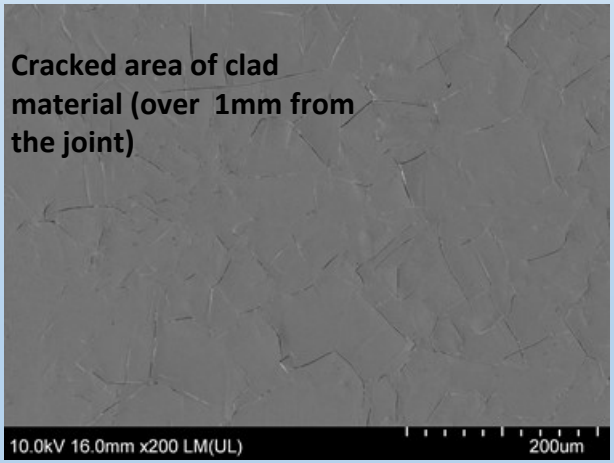

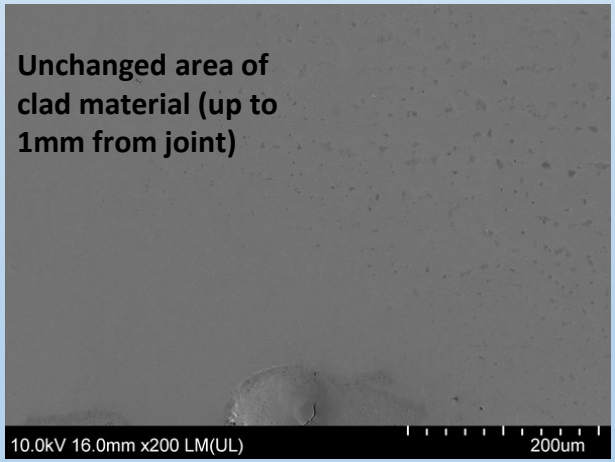

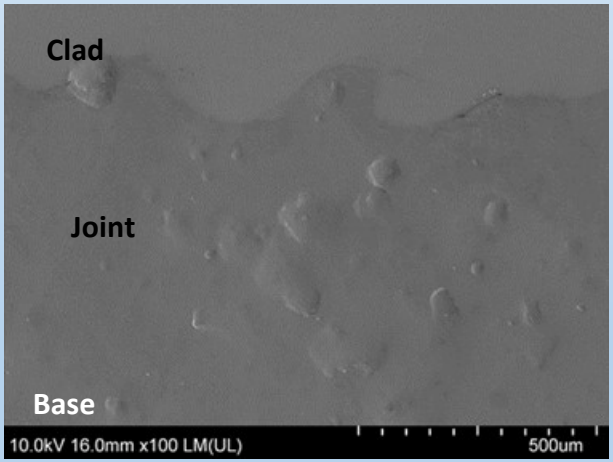

Sample 1.2 (annealed 610^{0}C) Base material: **P355NH**; Plate material: Inconel **C-276** after hydrogen charging. Area of clad material (up to 1000μm from the joint) remains unchanged

Microstructural observations after H charging

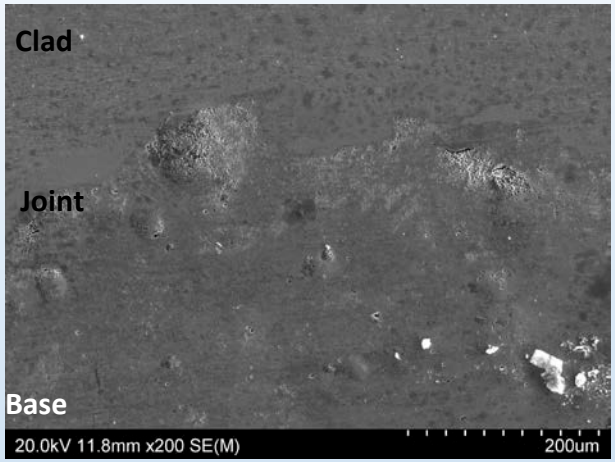

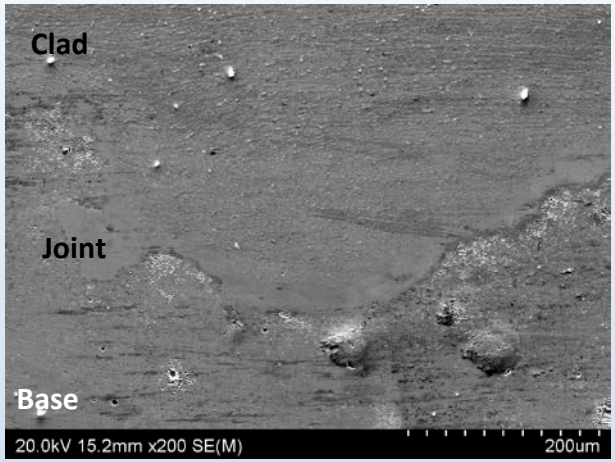

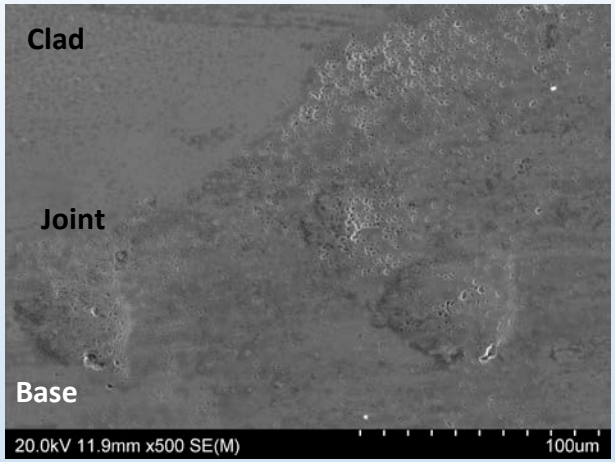

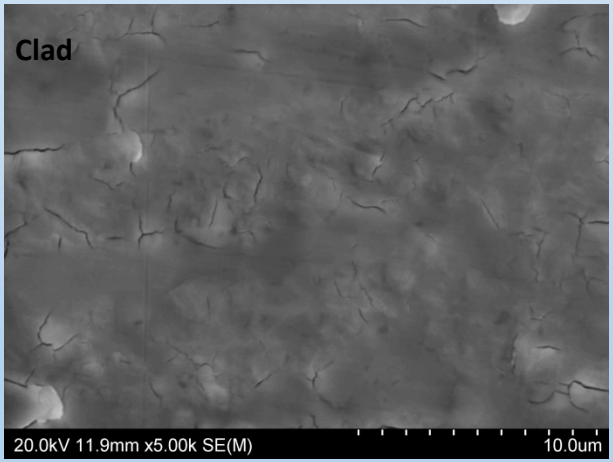

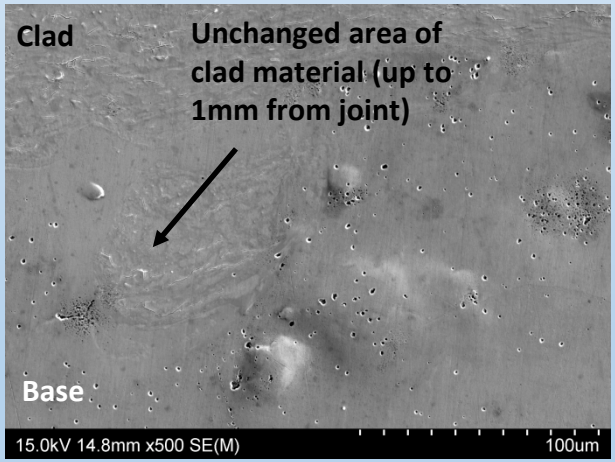

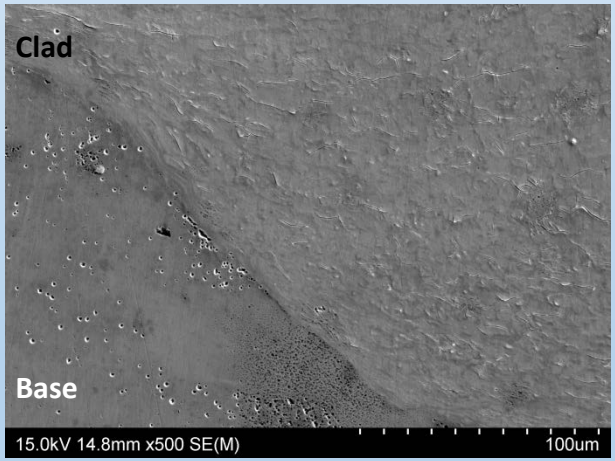

Sample 2.1, Base material: **P355NH**; Plate material: **SAF 2507,** austenitic-ferritic stainless steel.

Microstructural observations after H charging

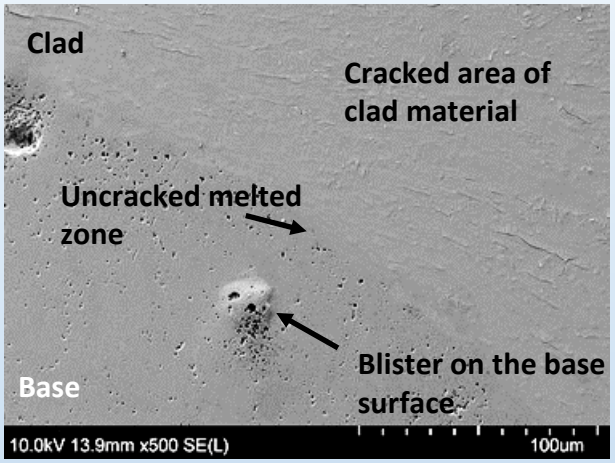

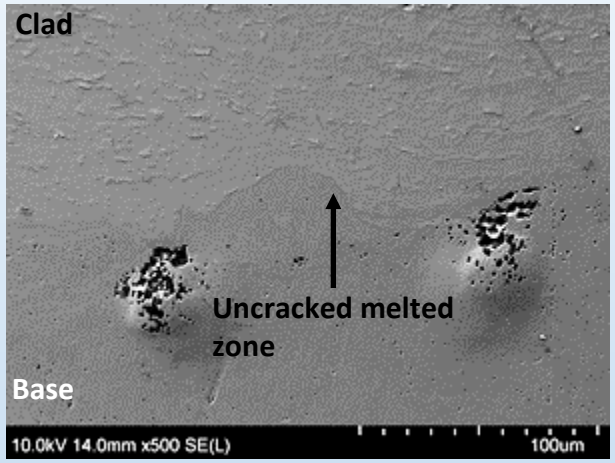

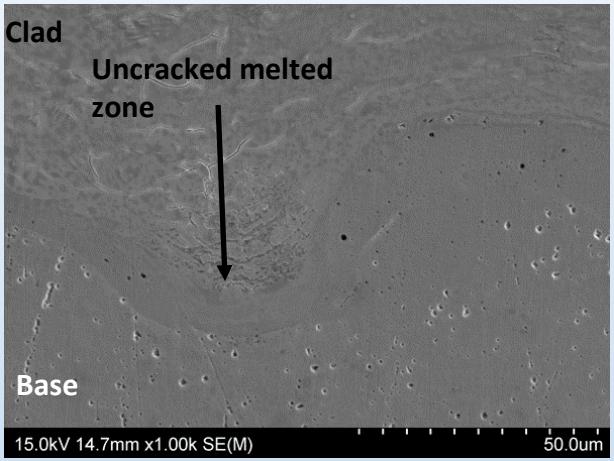

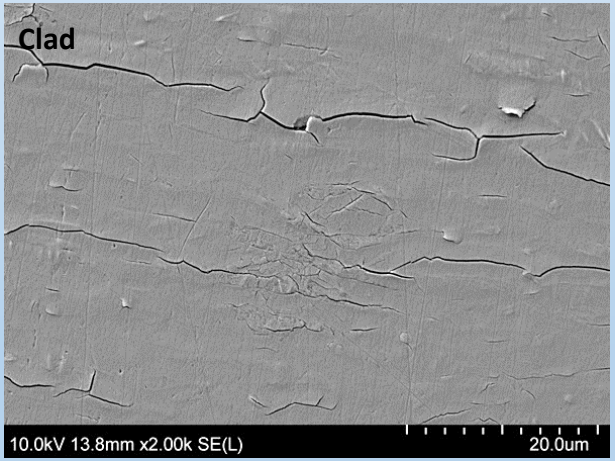

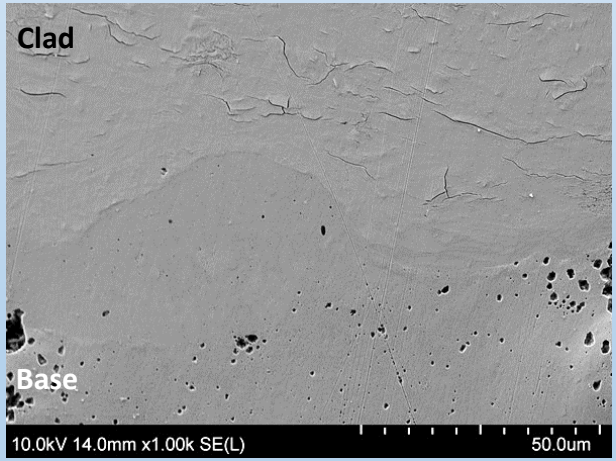

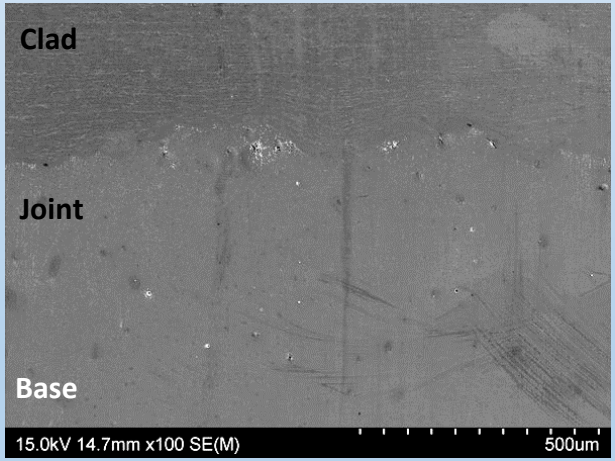

Sample 2.2 (annealed 610^{0}C), Base material: **P355NH**; Plate material: **SAF 2507,** austenitic-ferritic stainless steel

Shear test

Not charged

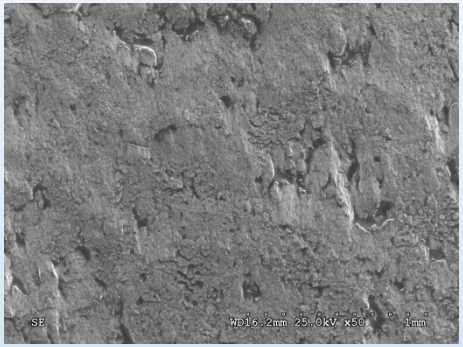

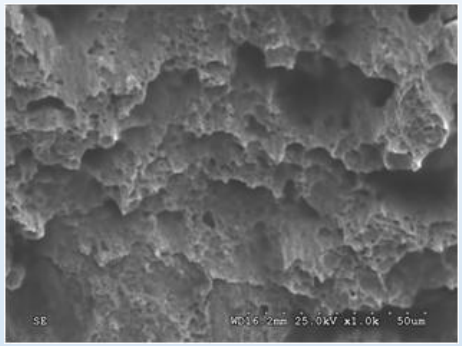

Sample 1.1

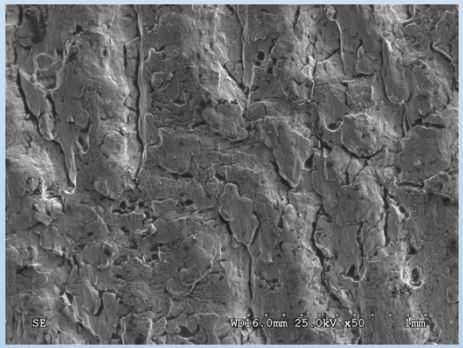

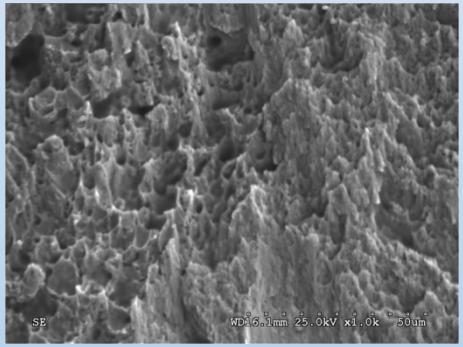

Sample 1.2

H charged

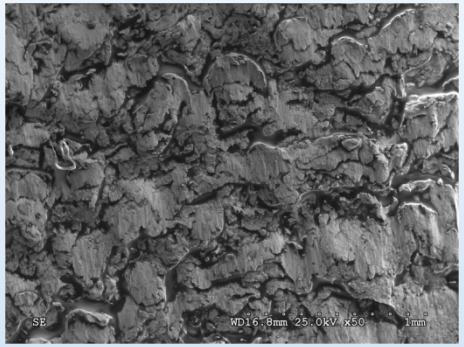

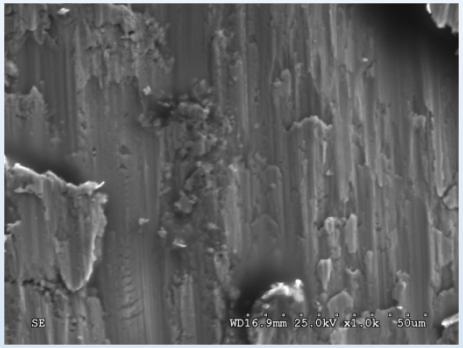

Sample 1.1

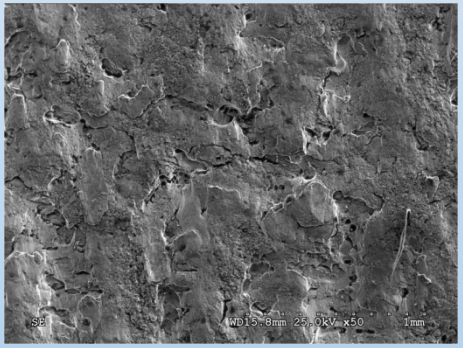

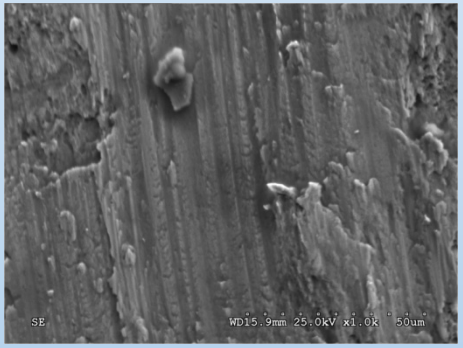

Sample 1.2

Shear test

Not charged

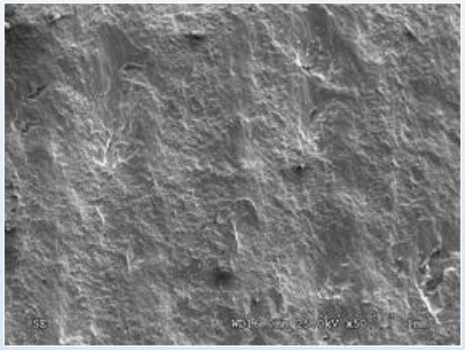

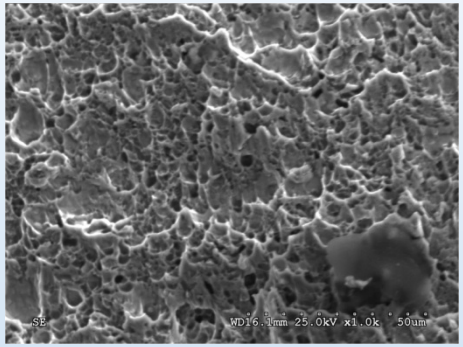

Sample 2.1

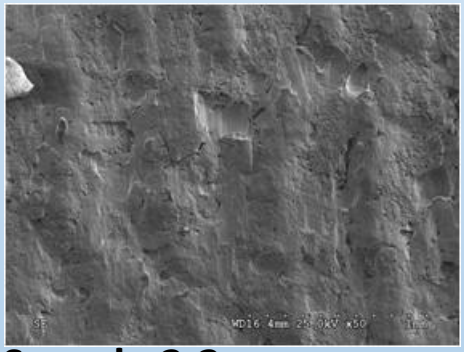

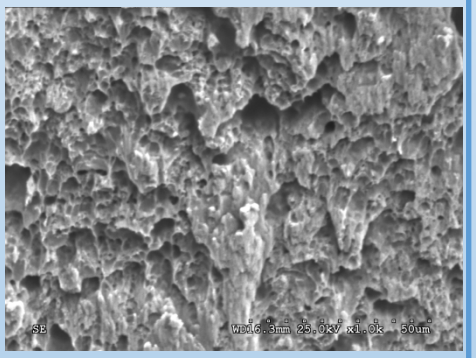

Sample 2.2

H charged

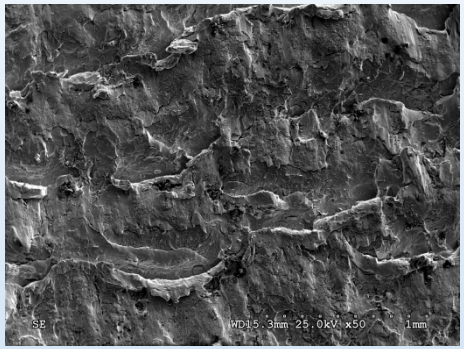

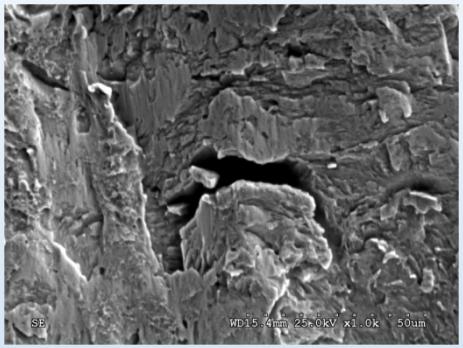

Sample 2.1

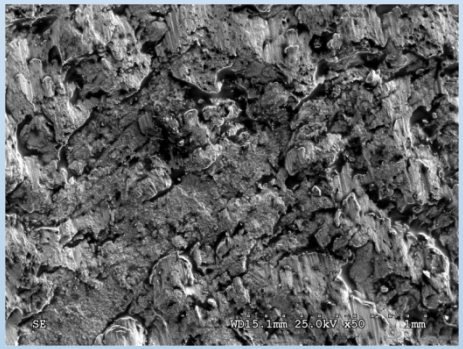

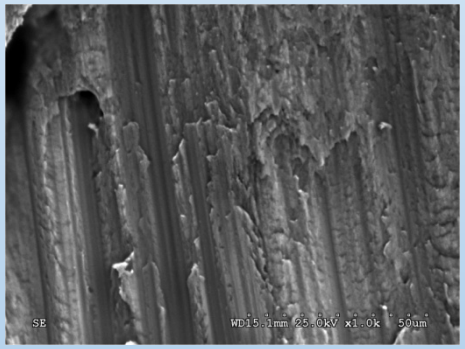

Sample 2.2

Shear test

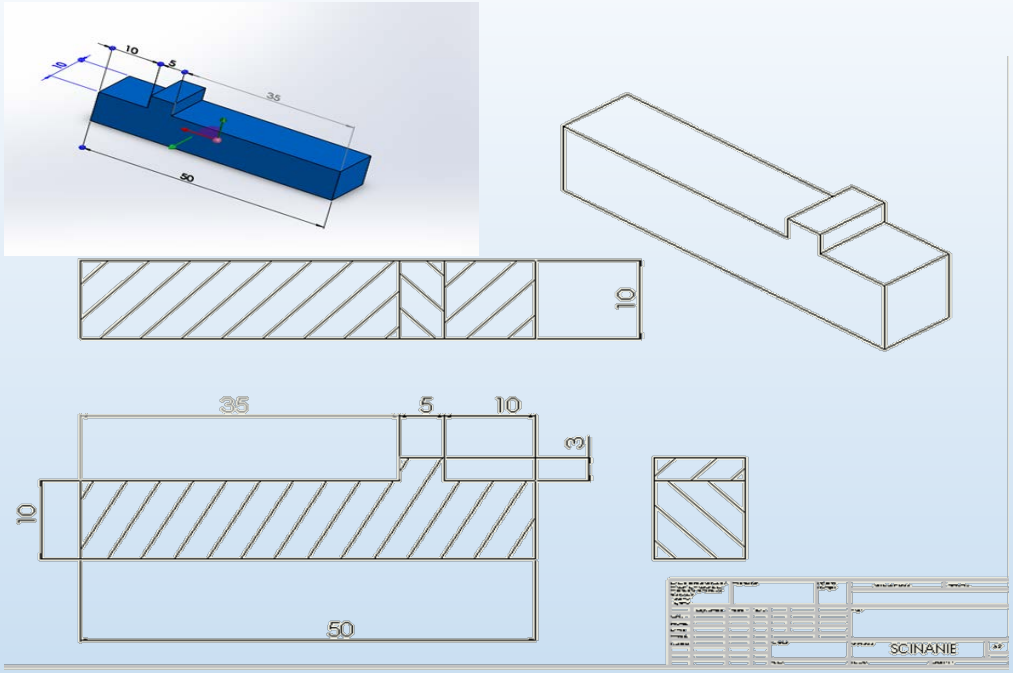

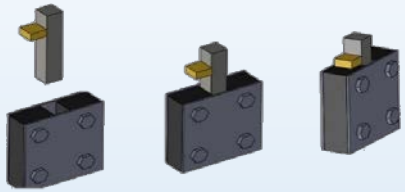

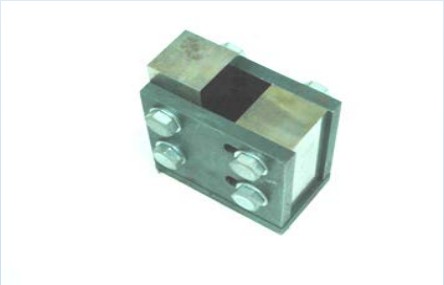

Shear test results

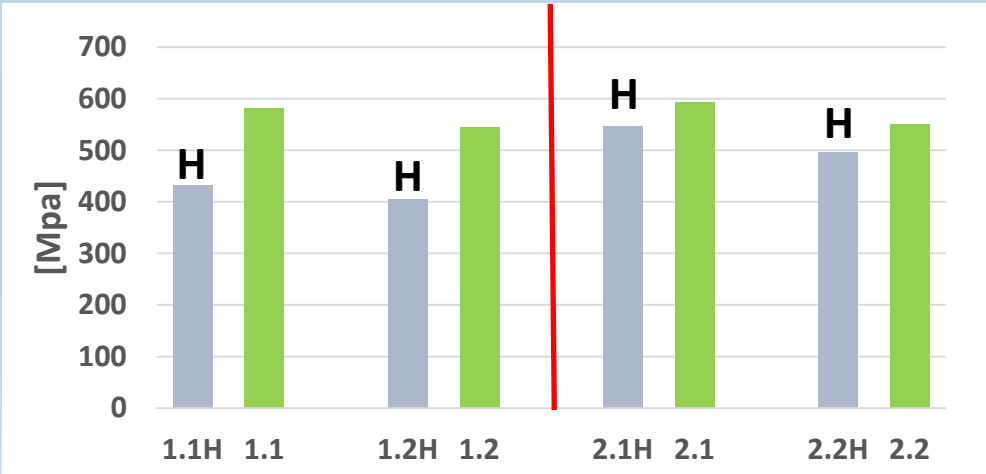

Average values for shear test for samples 1.1, 1.2 - 2.1 and 2.2 before and after hydrogen charging

Conclusions

- Obtained joints have wavy character what is typical fo explosive welding process.

- Hydrogen causes significant changes in microstructure in the flyer layer (surface microcracks and blisters) and base layer (blisters) of the investigated clad plates.

- In the process of explosive welding a strong deformation occurs adjacent to the joint. It is evidenced by the increased hardness of the metal near the joint and changing the shape of equiaxed grains in the elongated and refining of grains.

- Investigations of the local melted zones, formed at the interface of the explosively bonded low alloy and austenitic stainlss steels, have shown that the zones have an intermediate chemical composition, and exhibit in some case higher resistance to hydrogen corrosion than the bonded materials.

Conclusions

- **Hydrogen reduces the shear strength of investigated clads.**

- **Joints in which the bonded materials have an identical type crystal cells have similar rates and the solubility and diffusion of hydrogen, exhibit better mechanical properties in environments containing hydrogen.**

- **Strong microstructure changing, caused by explosion cladding, decreases susceptibility to increased hydrogen embritllement in the thin layer of ferritic corrosion resistance steels along the interface.**

THANK YOU ☺

www.materialresearch.eu